doi:10.1088/1742-6596/381/1/012041

Charge separation measurements in Pb–Pb collisions at LHC energies

Panos Christakoglou (for the ALICE Collaboration)

Nikhef, Science Park 105, 1098 XG Amsterdam, The Netherlands

E-mail: Panos.Christakoglou@nikhef.nl

Abstract. The prospect of observing parity violation from the strong interaction in relativistic heavy–ion collisions has recently gained great attention. We present the measurements of the azimuthal asymmetry of charged hadron production in Pb–Pb collisions at $\sqrt{s_{\rm NN}}=2.76$ TeV via the study of a parity even 3– and 2–particle azimuthal correlator. The results for LHC energies are compared to the ones reported by RHIC experiments but also to different models and to predictions from theory. The possible implications of these measurements to the local parity violation and the contribution from background effects are discussed.

1. Introduction

Heavy-ion collisions have been used extensively as a tool to study the phase transition from the nuclear matter to the deconfined state of quarks and gluons, the Quark-Gluon Plasma (QGP). It has been suggested recently that the hot and dense matter created in heavy-ion collisions may form metastable domains where the parity symmetry is locally violated [1]. This phenomenon is driven on one hand by the chiral symmetry restoration but also by the large (electro-) magnetic field produced in non-central heavy-ion collisions [2]. The maximum value of this magnetic field can reach levels of the order of 10^{15} T and its orientation lies in a direction that is perpendicular to the reaction plane. The combined effect of the chiral symmetry restoration, the magnetic field and the difference in the number of quarks with positive and negative chiralities (which is induced by their presence in a P-violating configuration) gives rise to the *Chiral Magnetic Effect*. The *Chiral Magnetic Effect* is reflected in a preferential same charge particle emission along the system's angular momentum. This leads to the separation of negatively and positively charged particles into two hemispheres separated by the reaction plane.

To study the effect, a 3-particle P-even azimuthal correlator has been proposed in [3]. This correlator is of the form:

$$\langle \cos(\phi_{\alpha} + \phi_{\beta} - 2\Psi_{RP}) \rangle,$$
 (1)

where $\phi_{\alpha,\beta}$ are the azimuthal angles of particles and Ψ_{RP} is the reaction plane angle. The brackets indicate a sum over all unique pairs or triplets for each event and then an average over all events. In practice the reaction plane angle that enters Eq. 1 for a given collision is not known, but it is rather estimated with the event plane reconstructed from the particle azimuthal distributions. Alternatively, in the three–particle correlation technique, the determination of the event plane is not required; instead, the role of the event plane is played by the third particle that enters the correlator with double the azimuth [3]. Under the assumption that particle c is correlated with the particles α and β and only via a common correlation to the reaction plane, we have:

1

doi:10.1088/1742-6596/381/1/012041

$$\langle cos(\phi_{\alpha} + \phi_{\beta} - 2\Psi_{RP})\rangle \times v_{2,c} = \langle cos(\phi_{\alpha} + \phi_{\beta} - 2\phi_{c})\rangle,$$
 (2)

In addition, a two-particle correlation analysis is performed based on the correlator:

$$\langle \cos(\phi_{\alpha} - \phi_{\beta}) \rangle,$$
 (3)

It is important to note that the main difference between the 2– and 3–particle correlators originates from the fact that the latter is not sensitive to background correlations not related to the reaction plane [3]. The former is sensitive to detector as well as non–flow effects.

In this article, we report the results for the two– and three–particle charge dependent azimuthal correlations with respect to the reaction plane for Pb–Pb collisions at $\sqrt{s_{\rm NN}} = 2.76$ TeV recorded in 2010 with ALICE [4] at the LHC.

2. Data analysis

The central tracking systems of ALICE [4], used in the present analysis are located inside a solenoidal magnet (B = 0.5 T); they provide full azimuth coverage within the pseudo-rapidity window $|\eta| < 0.9$. We used the following detector sub-systems: the *Inner Tracking System* (ITS) [4] and in particular the *Silicon Pixel Detectors* (SPD), the *Time Projection Chamber* (TPC) [5], the neutron *Zero Degree Calorimeter* (ZDC) and the VZERO detector [4]. The SPD are the two innermost layers of the ITS. The detector is used as part of the trigger, for calculation of the primary vertex but also for tracking. The TPC is the main tracking detector of the central barrel used also for particle identification. The VZERO detector consists of two arrays of 32 scintillators each, placed around the beam pipe on either side of the interaction region, covering the pseudo-rapidity ranges $2.8 < \eta < 5.1$ and $-3.7 < \eta < -1.7$, respectively [4]. Finally, the neutron ZDC of ALICE consists of two detectors located at about 114 m far from the interaction point on both the A- and the C-sides. More information about ALICE can be found in [4].

We analyzed data collected during the first LHC Pb–Pb runs in November–December 2010 at $\sqrt{s_{\mathrm{NN}}} = 2.76$ TeV. In total, we processed about 50 M minimum–bias events with the magnetic field B = 0.5 T. The event sample was split in two sets, based on the configuration of the polarity of the magnetic field. We analyzed each sample separately, and we considered the small differences in the results as part of our systematic uncertainty.

We considered events based on the online minimum—bias trigger, requiring two pixel chips hit in the outer layer of the SPD in coincidence with a signal from both sides of the VZERO detectors. We excluded empty triggers and beam background induced events (i.e. beam—gas or beam—halo) offline, using the timing information from the VZERO scintillators. We only considered events with a reconstructed primary vertex, thus reducing the number of surviving background (i.e. cosmic events with no reconstructed vertex) events. We restricted the vertex position within ± 7 cm along the beam axis, to ensure a uniform acceptance.

We estimated the centrality of the collision using the distribution of the signal from the VZERO scintillator detectors and fitting it with a Glauber model [6]. We investigated the dependence of the results on the usage of different centrality estimators (i.e. TPC tracks, SPD clusters) and we attributed the relevant differences to the systematic uncertainty. We analyzed the data in centrality classes which span the 0-80% fraction of the inelastic crosssection. In total, the number of events that passed all the above criteria were 15 M.

The tracks were reconstructed by the TPC, which provides a uniform acceptance which makes the corrections that need to be applied minimal (less than 2%). To select charged particles with high efficiency and to minimize the contribution from background tracks (i.e. secondary particles originating either from weak decays or from the interaction of particles with the material), we required all selected tracks to have at least 80 reconstructed space points out of the maximum 159 in the TPC. We accepted tracks having a $\langle \chi^2 \rangle$ of the fit per TPC cluster below 4 (two degrees

doi:10.1088/1742-6596/381/1/012041

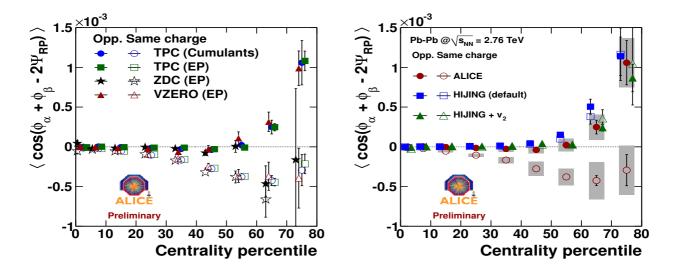


Figure 1. [Color online] Left: Centrality dependence of the integrated 3-particle correlator measured with four independent methods: the cumulants and the event plane estimate using the TPC, the ZDC and the VZERO detectors. Right: The centrality dependence of the integrated 3-particle correlator for ALICE (red points) compared to expectations from HIJING [7] with and without the inclusion of flow. In both plots the points are shifted along the x-axis to make them visible.

of freedom). We applied a cut on the distance of closest approach of the track to the primary vertex (dca), $d_0 < 3$ cm, to further reduce the contamination from background tracks. We investigated the effect of the contamination from such background tracks to our measurement by varying the cut on the dca; we also considered the relevant differences in these results in the evaluation of the systematic uncertainty. Finally, we accepted tracks in the phase space given by $|\eta| < 0.8$ and $0.2 < p_{\rm t} < 5.0$ GeV/c.

3. Results

We present in Fig. 1–left the centrality percentile dependence of the integrated 3–particle correlator, calculated with four independent analysis methods: the Q–cumulants using TPC tracks represented by the blue circles and the event plane estimate using the TPC (green squares) the ZDC (black stars) and the VZERO detector (red triangles). The full/open symbols correspond to the oppositely/same charge pairs, respectively. We observe a clear charge separation in the data between same and oppositely charge pairs. This separation is more pronounced when moving from central to peripheral collisions. In addition, the four independent methods agree quite well, indicating that the correlations and the corresponding charge separation we report are related to the orientation of the reaction plane.

We present the comparison of the experimental data to the expectations from HIJING [7] in Pb–Pb events at $\sqrt{s_{\mathrm{NN}}} = 2.76$ TeV in Fig. 1–right. We represent the statistical uncertainties in our measurement with the error bars, while the shaded areas correspond to the estimate of the systematic uncertainties. For the latter, we considered the following contributions: differences in the results from runs taken with different configurations of magnetic field polarities, variation of the cuts (both at the event and track level), different centrality estimators, the two charge combinations (positive–positive and negative–negative) for the correlations of same charge pairs and the differences in the results coming from the four independent analyses (Fig. 1– left). Still the biggest contribution to the shaded area originates from the uncertainty in the v₂ estimation entering in Eq. 2. For the v₂ estimation, the 2^{nd} and 4^{th} order Q–cumulants [8] were used,

doi:10.1088/1742-6596/381/1/012041

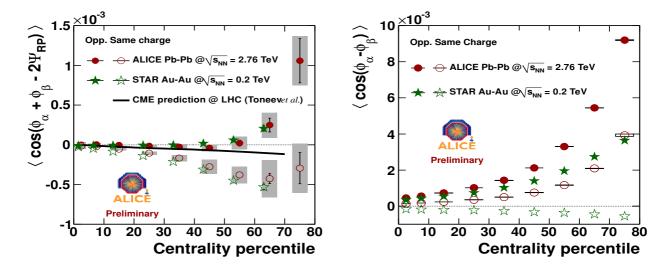


Figure 2. [Color online] (Left) The centrality dependence of the experimentally measured integrated 3–particle correlator for ALICE (red points) and STAR (green points). We shifted the STAR points along the x–axis to make them more visible. The solid line corresponds to a model prediction incorporating the *Chiral Magnetic Effect* for LHC energies [10]. (Right) The centrality dependence of the integrated 2–particle correlator for ALICE (red points) and STAR (green points).

each one being affected in a different way by both non-flow effects and flow fluctuations. The resulting $v_{2,c}$ was taken as the average of the two values, with half of the difference between $v_2\{2\}$ and $v_2\{4\}$ being attributed to the systematic uncertainty. The plot shows two sets of HIJING points, corresponding to the default version (blue squares) and the one coupled to a flow after-burner (green triangles). The latter provides the possibility to shuffle the distributions of generated particles based on the values of the experimentally measured differential v_2 for each centrality class [8]. HIJING predicts that the correlations between oppositely and same charged pairs will have not only the same sign (i.e. positive) but also the same magnitude within errors. In addition, the inclusion of the measured elliptic flow, does not alter either the strength or the sign of the correlations.

Figure. 2 presents the comparison of the centrality dependence of the integrated 3- (left plot) and 2-particle (right plot) correlators measured by ALICE in Pb-Pb collisions at $\sqrt{s_{\rm NN}}$ 2.76 TeV (red circles) and by STAR in Au–Au collisions at $\sqrt{s_{\rm NN}} = 0.2$ TeV (green stars) [9]. In both plots, the error bars correspond to the statistical uncertainties whereas we represent the systematic ones with the shaded areas. The full markers correspond to the correlations between oppositely charge pairs, with the open ones showing the same charge pairs. When looking at the 3-particle correlator, there is a remarkable agreement between the measurements at two different energies (note that we shifted the STAR points along the x-axis to make them more visible). We also compare our measurements to a prediction for the correlations of same charges from theory incorporating the *Chiral Magnetic Effect* [10] (black solid line). The version of this model, with its consideration of the duration and time evolution of the created magnetic field, clearly underestimates the observed magnitude of the correlations. The energy dependence of the Chiral Magnetic Effect is still a subject of great debate. In [10], the authors argue that the magnetic field developed in a heavy-ion collision at the LHC energies, although is significantly stronger than the one developed at RHIC energies, decays more rapidly. Since the time integral of the magnetic field is one of the key ingredients for the Chiral Magnetic Effect to develop, we

doi:10.1088/1742-6596/381/1/012041

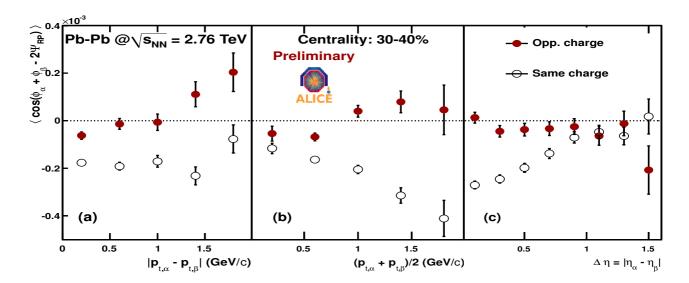


Figure 3. [Color online] The dependence of the 3-particle correlator on the: (a) p_t difference of the pair; (b) average p_t of the pair; (c) $\Delta \eta$ of the pair. The legend indicates the connection between the charge combinations and the different marker styles used.

would have expected a (significantly) smaller magnitude of the effect at the LHC with respect to RHIC. On the other hand, Kharzeev et al. already gave a hint that the magnitude of the effect might not change dramatically with energy in [11]. We present the centrality dependence of the 2–particle correlation analysis in Fig. 2–right. There is a change of sign in the correlations of same charged pairs between the LHC and RHIC energies, which could be interpreted in turn as a change of the correlation pattern in– and out–of–plane in the two experiments according to Koch et al. [12]. We believe that these arguments need to be reexamined considering the different sensitivity of the two techniques used on correlations not connected to the orientation of the reaction plane (e.g. non–flow contributions).

Analyzing the data in a more differential way, allows one to set constrains on the theoretical implementation behind this topic. We present in Fig. 3 the dependence of the 3-particle correlator on the p_t difference, the mean p_t and the pseudo-rapidity difference of the pair, in the left, middle and right plots, respectively. The open and full circles correspond to pairs having the same and opposite charge, respectively. In all plots, we show the results for the 30–40% centrality percentile. The opposite charged pairs show little or no dependence on either of the three variables used. On the other hand, the same charge pairs demonstrate a different pattern: the data points do not indicate a significant contribution from short range correlations (left plot), the magnitude of the correlations in absolute value seems to increase with increasing mean p_t of the pair (middle plot), whereas the $\Delta \eta$ dependence shows a width of one unit in $\Delta \eta$. We present in Fig. 4 the dependence of the 2-particle correlator on the $p_{\rm t}$ difference, the mean and the difference of the pseudo-rapidity of the pair, in the left, middle and right plots, respectively. We keep the same color and marker convention as in the previous plot. The stronger magnitude of the correlations between oppositely charge pairs is also observed in this representation. The correlations demonstrate a change in sign taking place around $\langle \Delta p_{\rm t} \rangle = 1.5$ and 3 GeV/c for the same and oppositely charge pairs, respectively (left plot). The mean η dependence demonstrate a triangular shape, the magnitude of which is more pronounced for more peripheral collisions (not shown) and for oppositely charge pairs. Both sets of data points demonstrate a strong contribution from short range correlations as seen in the pseudo-rapidity

doi:10.1088/1742-6596/381/1/012041

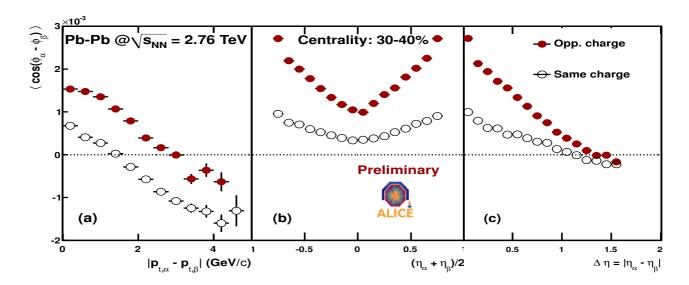


Figure 4. [Color online] The dependence of the 2-particle correlator on the: (a) $p_{\rm t}$ difference of the pair; (b) average η of the pair; (c) $\Delta \eta$ of the pair. The legend indicates the connection between the charge combinations and the different marker styles used.

difference dependence plot. Furthermore, the correlations indicate that they have a width of $\Delta \eta \approx 1$.

4. Summary

We reported the first measurement of the 2– and 3–particle correlators at the LHC energies with the ALICE experiment. The results of the 2–particle correlation analysis indicate that there is a change in the correlation pattern between LHC and RHIC energies. The integrated 3–particle correlator measured by ALICE shows a remarkable agreement with the published data from STAR, contrary to what one would naively expect taking into account the time integral of the magnetic field at both energies. We hope that these measurements, accompanied also by the relevant results of the differential analysis, will stimulate additional theoretical work on this topic. Finally, there were recent theoretical developments that demonstrate the importance of v_1 fluctuations [13] in these measurements considering also the small magnitude of the signal. The relevant contribution will be addressed and quantified in another publication.

5. References

- D. Kharzeev, R. D. Pisarski and M. H. G. Tytgat, Phys. Rev. Lett. 81, 512 (1998); D. Kharzeev and R. D. Pisarski, Phys. Rev. D61, 111901 (2000).
- [2] D. Kharzeev, Phys. Lett. B633, 260 (2006); K. Fukushima, D. E. Kharzeev and H. J. Warringa, Phys. Rev. D78, 074033 (2008).
- [3] S. A. Voloshin, Phys. Rev. C70, 057901 (2004).
- [4] K. Aamodt et al. [ALICE Collaboration], JINST 3, (2008) S08002.
- [5] J. Alme et al. [ALICE Collaboration], Nucl. Instrum. Meth. A622, (2010) 316.
- [6] B. Alver, M. Baker, C. Loizides, and P. Steinberg, (2008), arXiv:0805.4411 [nucl-ex].
- [7] M. Gyulassy and X.-N. Wang, Comput. Phys. Commun. 83, 307 (1994); X. N. Wang and M. Gyulassy, Phys. Rev. D44, 3501 (1991).
- [8] K. Aamodt et al. [ALICE Collaboration], Phys. Rev. Lett. 105, 252302 (2010).
- [9] J. Adams et al. [STAR Collaboration], Phys. Rev. Lett. 103, 251601 (2009); J. Adams et al. [STAR Collaboration], Phys. Rev. C81, 54908 (2010).
- [10] V. D. Toneev and V. Voronyuk, arXiv:1012.1508v1 [nucl-th].
- [11] D. Kharzeev et al., Nucl. Phys. **A803**, 227 (2008).
- [12] A. Bzdak et al., Phys.Rev. C81, 031901 (2010); A. Bzdak et al., Phys.Rev. C83, 014905 (2011).
- [13] D. Teaney and L. Yan, Phys. Rev. C83, 064904 (2011).